Research Article

Feasibility of Na^{18}F PET/CT and MRI for Noninvasive In Vivo Quantification of Knee Pathophysiological Bone Metabolism in a Canine Model of Post-traumatic Osteoarthritis

Maria I. Menendez, DVM, PhD[1], Bianca Hettlich, DrMedVet[1,2], Lai Wei, PhD[3], and Michael V. Knopp, MD, PhD[1]

Abstract

Purpose: To assess and quantify by molecular imaging knee osseous metabolic changes serially in an in vivo canine model of posttraumatic osteoarthritis (PTOA) of the knee utilizing sodium fluoride (Na^{18}F) positron emission tomography (PET)/computed tomography (CT) coregistered with magnetic resonance imaging (MRI).

Materials and Methods: Sodium fluoride PET imaging of 5 canines was performed prior to anterior cruciate ligament transection (ACLT) and 2 times post-ACLT (3 and 12 weeks). The PET/CT was coregistered with MRI, enabling serial anatomically guided visual and quantitative three-dimensional (3D) region of interest (ROI) assessment by maximum standardized uptake value.

Results: Prior to ACLT, every 3D ROI assessed in both knees showed no Na^{18}F uptake above background. The uptake of Na^{18}F in the bone of the ACLT knees increased exponentially, presenting significantly higher uptake at 12 weeks in every region compared to the ACLT knees at baseline. Furthermore, the uninjured contralateral limb and the ipsilateral distal bones and joints presented Na^{18}F uptake at 3 and 12 weeks post-ACLT.

Conclusion: This study demonstrated that Na^{18}F PET/CT coregistered with MRI is a feasible molecular imaging biomarker to assess knee osseous metabolic changes serially in an in vivo canine model of knee PTOA. Moreover, it brings a novel musculoskeletal preclinical imaging methodology that can provide unique insights into PTOA pathophysiology.

Introduction

Osteoarthritis (OA) is a leading cause of disability worldwide with age, obesity, and trauma or injury, representing major risk factors for disease development and progression.[1] One of the most common musculoskeletal traumatic injuries is disruption of the anterior cruciate ligament (ACL).[2] Young women performing pivoting sports, such as soccer and basketball, have a significantly higher risk of ACL injury than men.[3] Most patients with acute ACL tears are younger than 30 years of age at the time of their injury. As such, ACL injuries resulting in early-onset OA were associated with pain, functional limitations, and decreased quality of life. Reported incidence of posttraumatic osteoarthritis (PTOA) following ACL injury is as high as 87%.[3]

Individuals with ACL tears have a higher incidence of PTOA, approximately 50% between 10 and 20 years post-injury.[4] The increasing importance of comprehensive

[1] Department of Radiology, Wright Center of Innovation in Biomedical Imaging, The Ohio State University, Columbus, OH, USA
[2] Vetsuisse Faculty Bern, Bern, Switzerland
[3] Center for Biostatistics, The Ohio State University, Columbus, OH, USA

Corresponding Author:
Maria I. Menendez, Department of Radiology, The Wright Center of Innovation in Biomedical Imaging, The Ohio State University, 395 W 12th Avenue, Suite 400, Columbus, OH 43210, USA.
Email: menendez.59@osu.edu

noninvasive imaging of OA for diagnosis, prognosis, and follow-up is well recognized.

Although conventional radiography is the gold standard imaging technique for the evaluation of OA in clinical practice and in clinical trials, more sensitive imaging modalities are needed for the earlier diagnosis of PTOA.[5] It is now widely accepted that OA is a disease that affects all joint tissues. Currently, magnetic resonance imaging (MRI) is the preferred modality to assess early OA.[6] A comprehensive knee MRI examination includes only the knee joint, requires longer acquisition times, and fails to assess bone metabolism.[7] Sodium fluoride (Na[18]F) positron emission tomography (PET)/computed tomography (CT) provides an imaging alternative that detects molecular and cellular changes present in bone before morphological changes appear.[8-17] Because changes in bone metabolism are present long before morphological signs, Na[18]F can sooner identify and characterize early OA, allowing for quicker treatment and closer monitoring of disease progression.[9,18] There is evidence in the literature that Na[18]F PET was able to identify bone remodeling in the hip joint before morphological signs appeared on MRI.[9] Moreover, Na[18]F was able to detect metabolic abnormalities in subchondral bone in the knee that appeared normal on MRI.[19] Na[18]F as a bone metabolic tracer is currently primarily used for assessing skeletal metastasis in oncologic diagnosis and recently in cardiovascular calcifications. It has great potential for molecular musculoskeletal imaging, including OA and osteoporosis.[8-18,20-25]

Our group has used this canine model of knee PTOA and assessed early OA changes using ^{18}F-fluoro-D-glucose (F-FDG) PET.[26] Similar to coronary artery imaging, OA should include both assessment of inflammation (^{18}F-FDG) and calcium metabolism (Na[18]F).[8] Thus, ^{18}F-FDG and Na[18]F PET comprise excellent noninvasive in vivo molecular imaging biomarkers to evaluate the early pathophysiology of PTOA.[8] The uptake of Na[18]F in the bone is determined by vascular perfusion and bone surface accessibility for ion exchange, indirectly reflecting bone formation and bone resorption.[12] The advantages of Na[18]F PET/CT over conventional nuclear medicine techniques, such as Technetium 99m-methyl diphosphonate, to assess bone metabolism include higher sensitivity, superior resolution images, improved target to background ratio, and faster scan times.[15]

Current interest in the use of cross-sectional imaging techniques, and their multimodal combination in clinical practice, has led to combined hybrid modalities such as PET/CT and PET/MRI, largely because it enables intraindividual comparative studies. Combining functional and morphologic imaging for patients with OA have been lacking, and further studies are needed.

Surgically induced PTOA in the canine model has proved to be an excellent spontaneous model of disease. Furthermore, the canine knee (stifle) anatomy is markedly similar to that of humans.[27-35] The rationale for using this model is that ACL injury causes joint destabilization which subsequently leads to PTOA. The model imitates the degradation of the joint

structures after ACL rupture. The noninvasive anterior cruciate ligament transection (ACLT) canine model thus, constitutes a great fit for translational multimodal imaging utilizing human clinical MRI and PET scans.

Understanding how molecular imaging biomarkers are linked with early OA progression is critical to the development of targeted therapies, reducing the incidence and magnitude of premature joint disease and disability. Therefore, in this study, we assess the feasibility of a novel approach of Na[18]F PET/CT coregistered with MRI to detect and quantify pathological bone changes in this canine model of PTOA.

The aim of this study was to serially assess bone metabolism in a noninvasive in vivo canine model of knee PTOA. As such, we hypothesize that injury-induced inflammation induces bone molecular changes in the knee that undergoes ACLT compared to the contralateral knee. We further hypothesize that Na[18]F uptake will be increased in the contralateral knee after injury-induced trauma.

Materials and Methods

Study Design

Procedures were approved by the local University Institutional Laboratory Animal Care and Use Committee. Five (n = 5) healthy, skeletally mature male beagles (age 5 years; weighing 10-13 kg) were used. All dogs were without any clinical and radiological signs of orthopedic disorders. The dogs were individually housed in indoor pens and were fed a standard diet with water ad libitum.

Induction of OA

Dogs underwent general anesthesia induced by acepromazine (Vedco; Saint Joseph, Missouri; intravenously (IV), 0.2 mg/kg), ketamine (Ketaset; Fort Dodge Animal Health, Overland Park, Kansas; IV, 6 mg/kg), and diazepam (Valium; Roche, Madison, Wisconsin; IV, 0.35 mg/kg) and maintained by isoflurane (Iso-Flo; Abbott, Parsippany, New Jersey; infusion, 2%-4%). Bilateral knee arthroscopy using standard portals was performed to evaluate intra-articular structures. Using randomization, one knee had the anterior cruciate ligament transected, while the ACL in the contralateral knee was left intact (uninjured). The contralateral knee arthroscopy was performed to evaluate knee structures and to balance possible effects of the arthroscopy procedure itself, such as swelling or effusion, on postoperative knee imaging.

Positron Emission Tomography/Computed Tomography Imaging

Prior to, 3, and 12 weeks post-ACLT, under general anesthesia, the dogs underwent Na[18]F PET/CT. The patients were placed in supine position in a custom-made table with both knees extended into the designed custom-made foam knee coil, in order to mimic the same position as in the MRI knee coil and to facilitate MRI coregistration. The table and foam knee coil
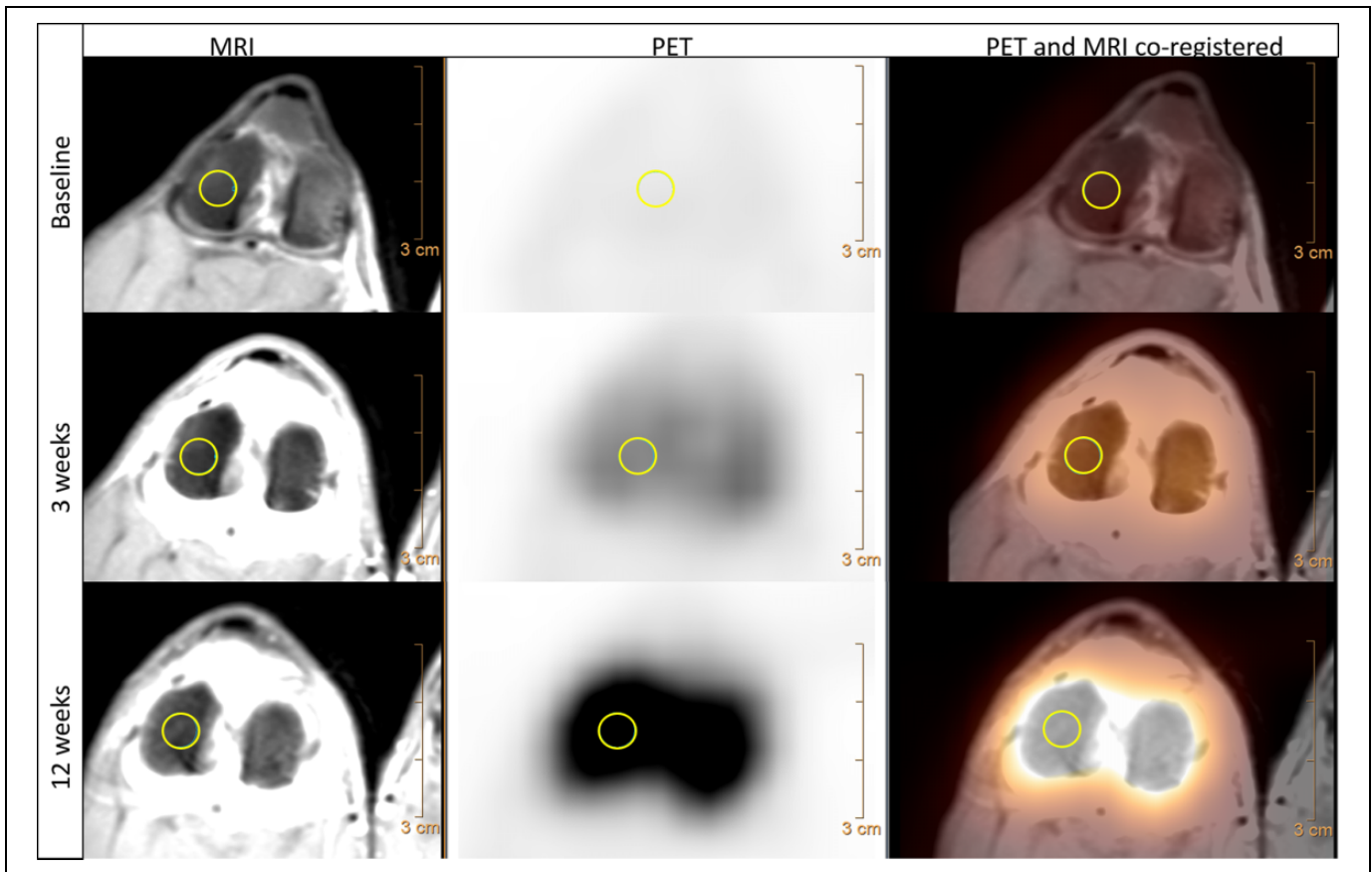
Figure 1. Representative knee MRI (proton density turbo spin-echo SPIR), Na[18]F PET, and Na[18]F PET/MRI coregistered (from left to right) axial views of the knee femoral condyles at baseline, 3 weeks, and 12 weeks post-ACLT (top to bottom), showing detailed knee morphology in the co-registered modalities. Showing Na[18]F background uptake at baseline, compared to higher uptake at 3 weeks, and significantly higher uptake at 12 weeks post-ACLT (bottom row). This elevated radioisotope uptake represented bone metabolism enhancement, caused by the injury-induced trauma. 3D regions of interest (6 mm) were manually traced over the lateral femoral condyle (yellow circles). ACLT indicates anterior cruciate ligament transection; 3D, three dimensional; MRI, magnetic resonance imaging; Na[18]F, sodium fluoride; PD, proton density; PET, positron emission tomography; SPIR, Spectral Presaturation with Inversion Recovery; TSE, turbo spin-echo.

positioning device together helped to consistently coregister both modalities. Sodium fluoride of 111 MBq (3 mCi) was injected in the cephalic vein via IV catheter. List mode time-of-flight raw data were acquired on the Gemini 64 TF with Astonish (Philips, Cleveland, Ohio) PET/CT system. Four millimeter (mm) isotropic voxel data sets (144×144 matrix size using a 576-mm field of view [FOV]) and 90 seconds/bed were reconstructed using the system default reconstruction parameters (3 iterations and 33 subsets). Computed tomography was acquired using the multislice helical system at 120 KVp, 163 mAs, and reconstructed with a 4-mm slice thickness, 512×512 matrix size, and 600-mm FOV for attenuation correction and coregistration. Whole-body static PET was acquired 30 minutes after 18F-NaF administration for a duration of 20 minutes (Figures 1–3).

Magnetic Resonance Imaging

Prior to, 3, and 12 weeks post-ACLT, under general anesthesia, the canines underwent MRI. A 3-T MRI human whole-body system (Achieva, Philips Healthcare, Cleveland, Ohio) equipped with an 8-channel knee coil was used. Dogs were placed in supine position, with both knees extended in the knee coil. A custom-made table was used to ensure the same position in both the MRI and the PET/CT. A clinical standard axial proton density (PD) turbo spin-echo (TSE) Spectral Presaturation with Inversion Recovery (SPIR) (Echo time [TE] = 15 ms, Repetition time [TR] = 2.1 seconds, flip angle = 90°, slice thickness = 2 mm, FOV = 115 mm, acquisition matrix 144×124, voxel size: FH = 0.56 mm, and AP = 0.7 mm) and a sagittal PD TSE fat saturated (TE = 45 ms, TR = 2.2 seconds, flip angle = 90°, slice thickness = 2 mm, and FOV = 88 mm) were acquired (Figure 1).

Analysis of PET/MRI

The PET/CT and MRI scans were performed in the same week for each time point and were coregistered using the Philips IntelliSpace Portal (version 6) workstation that uses an interpolation methodology to adjust for different matrix sizes. Three-dimensional (3D) regions of interest (ROIs) were traced
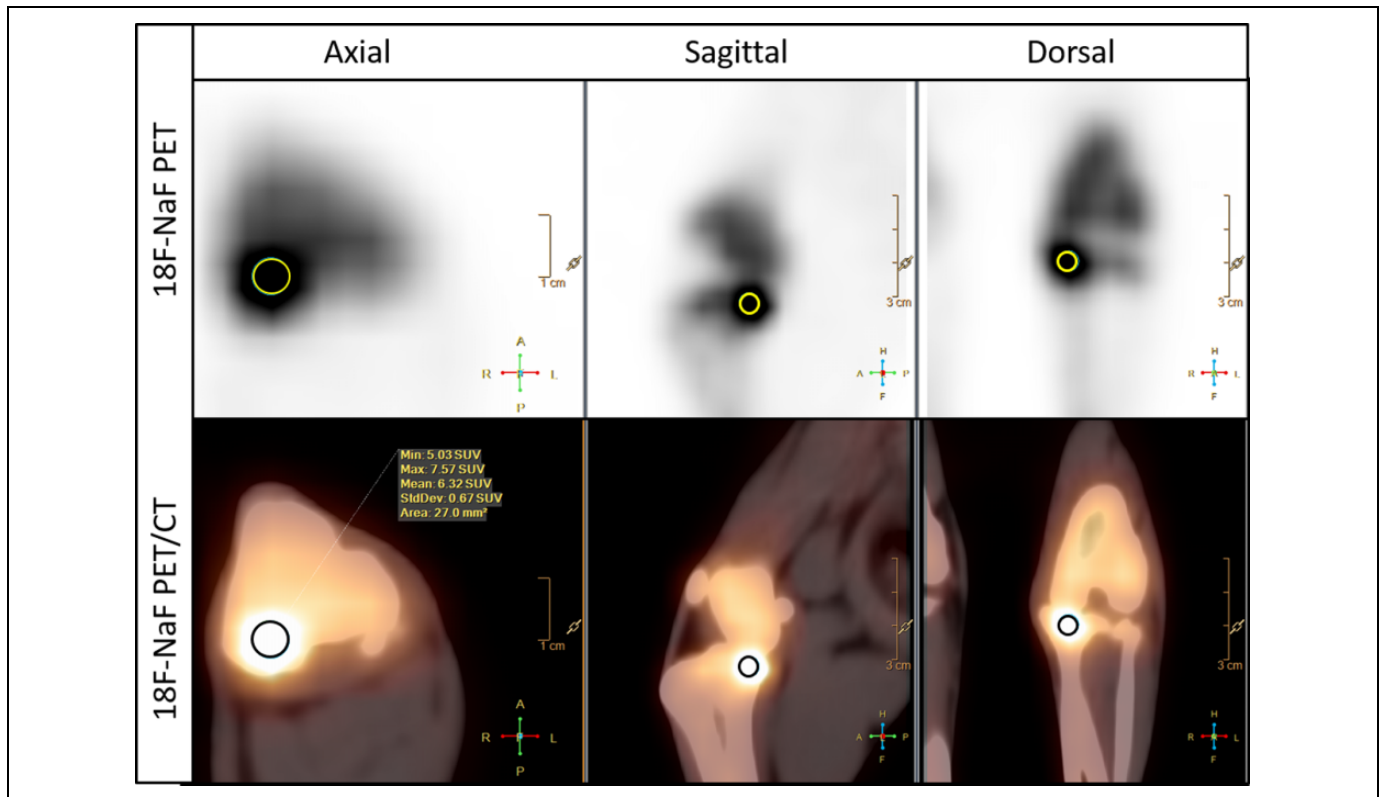
Figure 2. Representative Na^{18}F PET and Na^{18}F PET/CT views of a knee 12 weeks post-ACLT, showing higher Na^{18}F uptake of the 3D ROI in the medial tibia (yellow and black circles). This uptake represents bone metabolism changes and may be indicative of osteophyte formation. ACLT indicates anterior cruciate ligament transection; 3D, three dimensional; Na^{18}F, sodium fluoride; PET/CT, positron emission tomography/computed tomography; ROI, region of interest.

manually by an experienced veterinarian (MIM) to determine the SUV$_{max}$ in a consistent way. The 3D spheres of 6-mm diameter were traced for the lateral femoral condyle, medial femoral condyle, lateral tibia, and medial tibia (Figure 1).

Statistical Analyses

The linear mixed-effect model was used to study the association between the type of treatment (ACLT and uninjured) and the Na^{18}F SUV$_{max}$ at each ROI and time point of the PET images as well as the association of the Na^{18}F SUV$_{max}$ among the time points at each ROI for ACLT and uninjured, respectively. To determine the correlation within and between dogs, the Holm-Bonferroni method was used to adjust for multiplicity. P values <.05 were considered statistically significant. Statistical analysis was performed using SAS version 9.3 (SAS Institute, Cary, North Carolina).

Results

Both in vivo imaging modalities, Na^{18}F PET/CT and MRI, were successfully completed prior to, 3, and 12 weeks post-ACLT for all dogs and all image sets were successfully coregistered (Figure 1).

At baseline, before the induced injury was created, the knees had no pathological detectable uptake. Every 3D ROI assessed at baseline, in both knees, showed no Na^{18}F uptake above background, quantitatively verified using SUV$_{max}$ (Figures 1–4; Table 1).

At 12 weeks post-ACLT, all 3D ROIs assessed in the ACLT knees compared to the contralateral uninjured knees presented with significantly higher Na^{18}F SUV$_{max}$ uptake, including lateral and medial femur and tibia. The greatest uptake was detected at 12 weeks in the medial tibia region from the ACLT knees (Na^{18}F SUV$_{max}$ = 8.57 ± 0.66; mean ± standard error; Figures 3 and 4; Table 1).

At 3 weeks post-ACLT, the femur 3D ROIs in the ACLT knees, both lateral and femoral condyles, showed significantly higher Na^{18}F SUV$_{max}$ compared to the uninjured knees. The medial tibia followed a similar pattern, although it was not significantly different (Figures 3 and 4).

At 12 weeks, knees that underwent ACLT had significantly higher Na^{18}F uptake in every 3D ROI compared to the baseline. Interestingly, the medial femoral condyle ROIs also presented with increased significantly higher uptake at 3 and 12 weeks compared to the baseline (Figure 4; Table 2).

At 3 and/or 12 weeks post-ACLT, all dogs presented a visible, localized higher Na^{18}F uptake in the medial tibia of the ACLT knee (Figures 2 and 3).

Surprisingly, the Na^{18}F uptake was elevated in all assessed regions in the uninjured, contralateral knees at 12 weeks compared to the baseline. Although the substantial uptake was
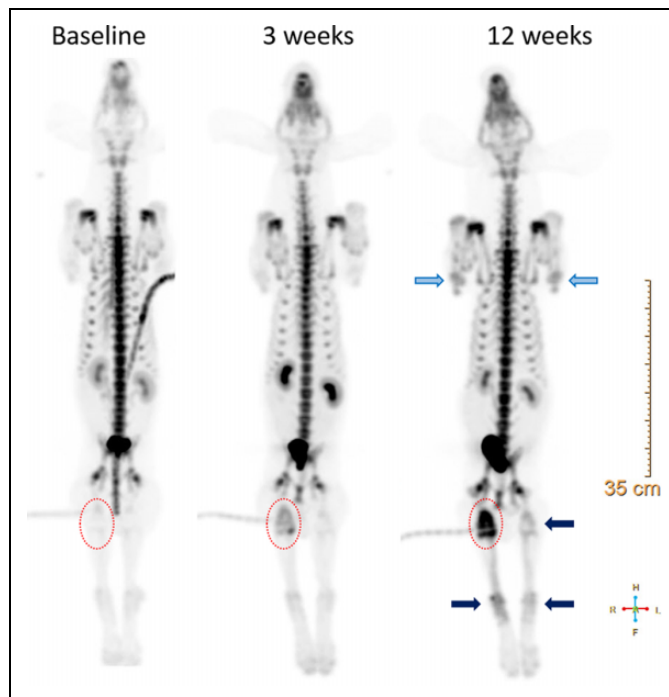
Figure 3. Representative whole-body static Na^{18}F PET at baseline, 3 weeks, and 12 weeks post-ACLT. Red circles show the exponential Na^{18}F uptake across time points in the knee that underwent ACLT, compared to the contralateral uninjured knee. At 12 weeks, the ipsilateral distal tibia, tarsal joints, and metatarsal bone (dark blue arrow) showed dramatic Na^{18}F uptake. Furthermore, the contralateral uninjured knee and distal joints (dark blue arrows) also had elevated Na^{18}F uptake. Additionally, the front limbs, carpal joints, and some metacarpal joints exhibited elevated tracer uptake (light blue arrows). ACLT indicates anterior cruciate ligament transection; Na^{18}F, sodium fluoride; PET, positron emission tomography.

visually observed, it was not statistically significant (Figures 3 and 4).

When assessing the static whole-body Na^{18}F PET at 12 weeks after injury-induced trauma in the ACLT knees, the ipsilateral distal tibia, tarsal joints, and metatarsal bone showed dramatic Na^{18}F uptake. Furthermore, the contralateral uninjured knee and distal joints also presented consistently with elevated Na^{18}F uptake. Additionally, in the front limbs, carpal joints and some metacarpal joints exhibited elevated tracer uptake (Figure 3).

Discussion

This study demonstrates the feasibility of Na^{18}F PET/CT co-registered with MRI as a novel diagnostic tool to quantify pathophysiological bone metabolism in an in vivo canine model of PTOA in the knee.

The incorporation of Na^{18}F into the bone matrix results in site-specific uptake in the knee joint, which enables not only uptake visualization but also a quantitative regional measurement (SUV$_{max}$) of pathological bone metabolism in a preclinical model of PTOA.

At baseline, prior to ACLT, no Na^{18}F uptake was detectable in the healthy canine knees. This finding is consistent with a similar arthritis study in a murine model.[13] Our observation differs from the murine study regarding the time point at which the increased uptake and increased bone metabolism was noted. In the murine model, the uptake decreased at 5 weeks, whereas in our canine model, the uptake increased exponentially, reaching highest uptake at 12 weeks.

All the regions of interest from the ACLT knees had significantly higher Na^{18}F uptake compared to the uninjured knees at 12 weeks. This result may be related to the increased rate of remodeling, which has been shown in an ACLT canine model of OA, where thinning of the subchondral plate occurs.[36,37] The increased incorporation of Na^{18}F into the bone matrix was greater at 12 weeks than 3 weeks postinjury. This finding is consistent with current studies in OA bone pathogenesis, where OA subchondral bone remodeling is biphasic. In the early stage, there is increased bone remodeling, and as the OA progresses, the remodeling decreases while bone formation increases.[38]

Whole-body static Na^{18}F PET allowed us to detect bone metabolic changes in the whole body. We expected to see bone metabolic changes with minor tracer uptake in the contralateral uninjured knees due to the instability created by the ACL transection. We also observed ^{18}F-FDG uptake in our previous study, presenting a different radiotracer uptake pattern, showing higher ^{18}F-FDG uptake 3 weeks post-ACLT, in contrast to the higher Na^{18}F uptake at 12 weeks presented in this study. These findings are consistent with the concept that ^{18}F-FDG is trapped in cells after phosphorylation, presenting inflammation due to increased glucose metabolism.[26] A different pattern is showed with Na^{18}F, which accumulates in the bone when bone remodeling is increased. Both molecular imaging biomarkers complement each other to provide a deeper insight into early knee PTOA pathogenesis.

The higher Na^{18}F uptake observed in the medial tibia of the ACLT knees at 3 weeks (4 dogs) and 12 weeks (5 dogs) may be indicative of increased bone perfusion and highly significant bone formation (osteophytes).

Surprisingly, several bones and joints presented higher uptake, including the ipsilateral distal tibia, tarsal joint, and metatarsal bone, and, to a lesser extent, the contralateral bones and joints. Moreover, carpal joints and some metacarpal joints in the front limbs exhibited elevated tracer uptake. These findings may reveal a systemic effect created by transecting the ACL, rather than altered gait mechanics due to joint instability.

Arthroscopic surgery was chosen to produce joint injury minimizing the profound effects of arthrotomy, which may lead to substantial synovitis, hemorrhage, joint capsular fibrosis, and associated pain and dysfunction. The canine model is one of the most common studied species with respect to spontaneous models of OA due to the knee similarity to humans.[28]

It is important to mention some limitations of this study. The contralateral knee joint was used as the uninjured comparison, instead of using nonoperated control dogs. Using the uninjured contralateral knee helped to minimize interanimal variation.
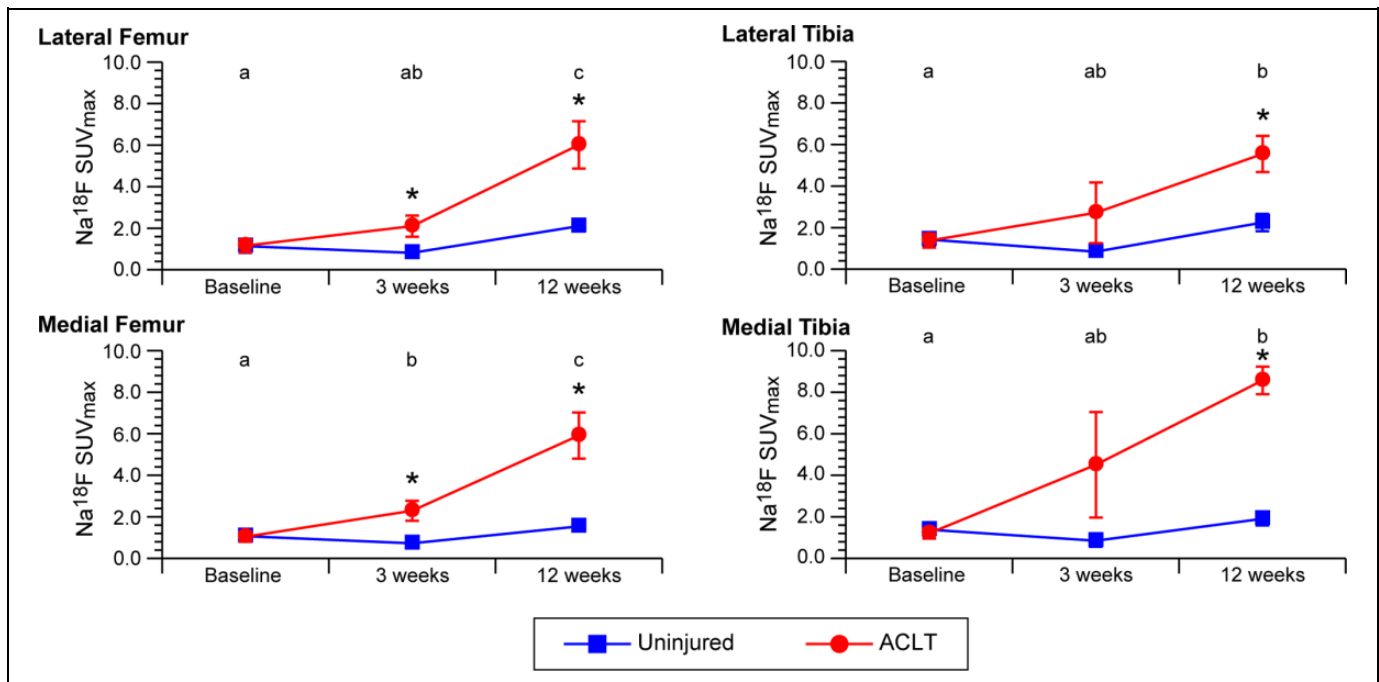
Figure 4. ROI Na^{18}F SUV$_{max}$ from the ACLT and uninjured knees at baseline, 3 weeks, and 12 weeks. Data were expressed as mean ± SEM. Different letters comparing ACLT ROIs across time (a, b, and c) differ significantly (*P* < .05). Asterisks (*) showed significant difference between ACLT and uninjured knees. ACLT indicates anterior cruciate ligament transection; Na^{18}F, sodium fluoride; ROI, region of interest; SEM, standard error of the mean; SUV$_{max}$, maximum standardized uptake value.

Table 1. Na^{18}F Maximum Standardized Uptake Values (SUV$_{max}$) of 3D Regions of Interest (ROIs) in the ACLT and Uninjured Knee at Baseline, 3 Weeks, and 12 Weeks Post-ACLT.

Assessed ROI	Timeline	ACLT Na^{18}F SUV$_{max}$ (Mean ± SE)	Uninjured Na^{18}F SUV$_{max}$ (Mean ± SE)	Linear Mixed Model *P* Value
Lateral femur	Baseline	1.16 ± 0.32	1.15 ± 0.32	.93
	3 weeks	2.10 ± 0.51	0.82 ± 0.13	.03[a]
	12 weeks	6.01 ± 1.14	2.11 ± 0.25	.01[a]
Medial femur	Baseline	1.04 ± 0.24	1.08 ± 0.26	.60
	3 weeks	2.29 ± 0.48	0.73 ± 0.08	.02[a]
	12 weeks	5.91 ± 1.11	1.55 ± 0.25	.01[a]
Lateral tibia	Baseline	1.37 ± 0.34	1.42 ± 0.30	1.00
	3 weeks	2.72 ± 1.46	0.84 ± 0.22	.34
	12 weeks	5.55 ± 0.87	2.24 ± 0.41	.001[a]
Medial tibia	Baseline	1.20 ± 0.26	1.39 ± 0.30	.09
	3 weeks	4.50 ± 2.54	0.86 ± 0.29	.14
	12 weeks	8.57 ± 0.66	1.91 ± 0.32	<.001[a]

Abbreviations: ACLT, anterior cruciate ligament transection; 3D, three dimensional; Na^{18}F, sodium fluoride; SE, standard error.
[a]*P* < .05 considered significant.

Table 2. Na^{18}F Maximum Standardized Uptake Values (SUV$_{max}$) of 3D Regions of Interest (ROIs) in the ACLT Knee at Baseline (BL), 3 Weeks, and 12 Weeks Post-ACLT, and Multiple Comparisons *P* Values Using Holm-Bonferroni.

Assessed ROI	Timeline	ACLT Na^{18}F SUV$_{max}$ (Mean ± SE)	Holm-Bonferroni *P* Value
Lateral femur	3 weeks vs BL	0.94 ± 0.57	.12
	12 weeks vs BL	4.85 ± 1.39	.01[a]
	12 vs 3 weeks	3.91 ± 1.45	.04[a]
Medial femur	3 weeks vs BL	1.25 ± 0.53	.04[a]
	12 weeks vs BL	4.87 ± 1.31	.01[a]
	12 vs 3 weeks	3.62 ± 1.35	.04[a]
Lateral tibia	3 weeks vs BL	1.34 ± 1.23	.59
	12 weeks vs BL	4.17 ± 1.15	.01[a]
	12 vs 3 weeks	2.83 ± 1.88	.31
Medial tibia	3 weeks vs BL	3.30 ± 2.39	.39
	12 weeks vs BL	7.36 ± 0.77	<.001[a]
	12 vs 3 weeks	4.06 ± 2.58	.28

Abbreviations: ACLT, anterior cruciate ligament transection; 3D, three dimensional; Na^{18}F, sodium fluoride; SE, standard error.
[a]*P* < .05 considered significant.

The study finalized 12 weeks post-ACLT. Longer studies will help provide greater longitudinal data in early PTOA. The purpose of coregistering MRI to Na^{18}F PET/CT in this study was to be able to compare both molecular imaging biomarker studies. Magnetic resonance imaging analysis is not presented in this report to focus on Na^{18}F PET. Magnetic resonance imaging was only used for localizing purposes and to keep consistency when compared to previous studies done with the

same protocol. Histopathology was beyond the scope of this article; thus, we cannot comment on the correlation between higher uptake and bone pathology. Alternatively, we described the abnormal bone changes. Further studies are needed with a larger dog population to elucidate the different calcium metabolic changes that we observed in the knees, additional bones, and joints. Future studies will benefit from supplemental blood biodistribution analyses. Furthermore, $Na^{18}F$ dose reduction and reconstruction optimization should be examined in future studies to minimize radiation exposure levels to as low as reasonably achievable (ALARA).

We demonstrate the potential of $Na^{18}F$ PET/CT coregistered with MRI to monitor serially and to quantify pathological bone changes in this canine model of knee PTOA. Jointly, with our previous ^{18}F-FDG observations in the same canine model, we present a noninvasive multimodal imaging methodology to investigate the pathophysiology of OA through molecular imaging biomarkers ($Na^{18}F$ and ^{18}F-FDG), where bone changes and inflammation are the major parameters used to assess early PTOA. This preclinical model may provide new insights into PTOA pathogenesis and lead to new OA targets than could be translated to young adult patients to treat OA progression.

References

1. Cross M, Smith E, Hoy D, et al. The global burden of hip and knee osteoarthritis: estimates from the global burden of disease 2010 study. *Ann Rheum Dis*. 2014;73(7):1323–1330.
2. Frobell RB, Lohmander LS, Roos HP. Acute rotational trauma to the knee: poor agreement between clinical assessment and magnetic resonance imaging findings. *Scand J Med Sci Sports*. 2007;17(2):109–114.
3. Friel NA, Chu CR. The role of ACL injury in the development of posttraumatic knee osteoarthritis. *Clin Sports Med*. 2013;32(1):1–12.
4. Lohmander LS, Englund PM, Dahl LL, Roos EM. The long-term consequence of anterior cruciate ligament and meniscus injuries: osteoarthritis. *Am J Sports Med*. 2007;35(10):1756–1769.
5. Eagle S, Potter HG, Koff MF. Morphologic and quantitative magnetic resonance imaging of knee articular cartilage for the assessment of post-traumatic osteoarthritis. *J Orthop Res*. 2017;35(3):412–423.
6. Boesen M, Ellegaard K, Henriksen M, et al. Osteoarthritis year in review 2016: imaging. *Osteoarthritis cartilage. 2016*.2017;25(2):216–226.
7. Guermazi A, Roemer FW, Crema MD, Englund M, Hayashi D. Imaging of non-osteochondral tissues in osteoarthritis. *Osteoarthritis Cartilage*. 2014;22(10):1590–1605.
8. Raynor W, Houshmand S, Gholami S, et al. Evolving role of molecular imaging with (18)F-sodium fluoride PET as a biomarker for calcium metabolism. *Curr Osteoporos Rep*. 2016;14(4):115–125.
9. Kobayashi N, Inaba Y, Tateishi U, et al. Comparison of 18F-fluoride positron emission tomography and magnetic resonance imaging in evaluating early-stage osteoarthritis of the hip. *Nucl Med Commun*. 2015;36(1):84–89.
10. Dyke JP, Synan M, Ezell P, Ballon D, Racine J, Aaron RK. Characterization of bone perfusion by dynamic contrast-enhanced magnetic resonance imaging and positron emission tomography in the Dunkin-Hartley guinea pig model of advanced osteoarthritis. *J Orthop Res*. 2015;33(3):366–372.
11. Blake GM, Park-Holohan SJ, Cook GJ, Fogelman I. Quantitative studies of bone with the use of 18F-fluoride and 99mTc-methylene diphosphonate. *Semin Nucl Med*. 2001;31(1):28–49.
12. Frost ML, Blake GM, Park-Holohan SJ, et al. Long-term precision of 18F-fluoride PET skeletal kinetic studies in the assessment of bone metabolism. *J Nucl Med*. 2008;49(5):700–707.
13. Irmler IM, Gebhardt P, Hoffmann B, et al. 18 F-Fluoride positron emission tomography/computed tomography for noninvasive in vivo quantification of pathophysiological bone metabolism in experimental murine arthritis. *Arthritis Res Ther*. 2014;16(4):R155.
14. Umemoto Y, Oka T, Inoue T, Saito T. Imaging of a rat osteoarthritis model using (18)F-fluoride positron emission tomography. *Ann Nucl Med*. 2010;24(9):663–669.
15. Iagaru A, Mittra E, Dick DW, Gambhir SS. Prospective evaluation of (99 m)Tc MDP scintigraphy, (18)F NaF PET/CT, and (18)F FDG PET/CT for detection of skeletal metastases. *Mol Imaging Biol*. 2012;14(2):252–259.
16. Blau M, Ganatra R, Bender MA. 18 F-fluoride for bone imaging. *Semin Nucl Med*. 1972;2(1):31–37.
17. Blau M, Nagler W, Bender MA. Fluorine-18: a new isotope for bone scanning. *J Nucl Med*. 1962;3:332–334.
18. Kobayashi N, Inaba Y, Tateishi U, et al. New application of 18F-fluoride PET for the detection of bone remodeling in early-stage osteoarthritis of the hip. *Clin Nucl Med*. 2013;38(10):e379–e383.
19. Kogan F, Fan AP, McWalter EJ, Oei EH, Quon A, Gold GE. PET/MRI of metabolic activity in osteoarthritis: a feasibility study. *J Magn Reson Imaging*. 2017;45(6):1736–1745.
20. Grant FD, Fahey FH, Packard AB, Davis RT, Alavi A, Treves ST. Skeletal PET with 18F-fluoride: applying new technology to an old tracer. *J Nucl Med*. 2008;49(1):68–78.
21. Azad GK, Taylor B, Rubello D, Colletti PM, Goh V, Cook GJ. Molecular and functional imaging of bone metastases in breast

and prostate cancers: an overview. *Clin Nucl Med*. 2016;41(1):
e44–e50.

22. Pawade TA, Cartlidge TR, Jenkins WS, et al. Optimization and reproducibility of aortic valve 18F-fluoride positron emission tomography in patients with aortic stenosis. *Circ Cardiovasc Imaging*. 2016;9(10):e005131.

23. Cheng C, Heiss C, Dimitrakopoulou-Strauss A, et al. Evaluation of bone remodeling with (18)F-fluoride and correlation with the glucose metabolism measured by (18)F-FDG in lumbar spine with time in an experimental nude rat model with osteoporosis using dynamic PET-CT. *Am J Nucl Med Mol Imaging*. 2013;3(2): 118–128.

24. Siddique M, Blake GM, Frost ML, et al. Estimation of regional bone metabolism from whole-body 18F-fluoride PET static images. *Eur J Nucl Med Mol Imaging*. 2012;39(2):337–343.

25. Bruijnen ST, van der Weijden MA, Klein JP, et al. Bone formation rather than inflammation reflects ankylosing spondylitis activity on PET-CT: a pilot study. *Arthritis Res Ther*. 2012;14(2):R71.

26. Menendez MI, Hettlich B, Wei L, Knopp MV. Preclinical multimodal molecular imaging using 18F-FDG PET/CT and MRI in a phase I study of a knee osteoarthritis in in vivo canine model. *Mol Imaging*. 2017;16. doi:10.1177/1536012117697443.

27. Kuyinu EL, Narayanan G, Nair LS, Laurencin CT. Animal models of osteoarthritis: classification, update, and measurement of outcomes. *J Orthop Surg Res*. 2016;11(1):19.

28. Cook JL, Kuroki K, Visco D, Pelletier JP, Schulz L, Lafeber FP. The OARSI histopathology initiative—recommendations for histological assessments of osteoarthritis in the dog. *Osteoarthritis Cartilage*. 2010;18(suppl 3):S66–S79.

29. Boileau C, Martel-Pelletier J, Abram F, et al. Magnetic resonance imaging can accurately assess the long-term progression of knee structural changes in experimental dog osteoarthritis. *Ann Rheum Dis*. 2008;67(7):926–932.

30. Lampropoulou-Adamidou K, Lelovas P, Karadimas EV, et al. Useful animal models for the research of osteoarthritis. *Eur J Orthop Surg Traumatol*. 2014;24(3):263–271.

31. Batiste DL, Kirkley A, Laverty S, et al. High-resolution MRI and micro-CT in an ex vivo rabbit anterior cruciate ligament transection model of osteoarthritis. *Osteoarthritis Cartilage*. 2004;12(8): 614–626.

32. Innes JF, Costello M, Barr FJ, Rudorf H, Barr AR. Radiographic progression of osteoarthritis of the canine stifle joint: a prospective study. *Vet Radiol Ultrasound*. 2004;45(2):143–148.

33. D'Anjou MA, Moreau M, Troncy E, et al. Osteophytosis, subchondral bone sclerosis, joint effusion and soft tissue thickening in canine experimental stifle osteoarthritis: comparison between 1.5 T magnetic resonance imaging and computed radiography. *Vet Surg*. 2008;37(2):166–177.

34. Libicher M, Ivancic M, Hoffmann M, Wenz W. Early changes in experimental osteoarthritis using the Pond-Nuki dog model: technical procedure and initial results of in vivo MR imaging. *Eur Radiol*. 2005;15(2):390–394.

35. Pujol E, Van Bree H, Cauzinille L, Poncet C, Gielen I, Bouvy B. Anatomic study of the canine stifle using low-field magnetic resonance imaging (MRI) and MRI arthrography. *Vet Surg*. 2011;40(4):395–401.

36. Sniekers YH, Intema F, Lafeber FP, et al. A role for subchondral bone changes in the process of osteoarthritis; a micro-CT study of two canine models. *BMC Musculoskelet Disord*. 2008;9:20.

37. Intema F, Sniekers YH, Weinans H, et al. Similarities and discrepancies in subchondral bone structure in two differently induced canine models of osteoarthritis. *J Bone Miner Res*. 2010;25(7):1650–1657.

38. Burr DB, Gallant MA. Bone remodelling in osteoarthritis. *Nat Rev Rheumatol*. 2012;8(11):665–673.